Narrow Beam Lithium Niobate Antenna Utilizing Subwavelength Structure for Optical Phased Array

Shuhang Zheng
College of Optical Science and Engineering
Zhejiang University
Hangzhou, China
zhengsh@zju.edu.cn

Kaiyang Yuan
College of Optical Science and Engineering
Zhejiang University
Hangzhou, China
gdyuankaiyang@zju.edu.cn

Jintao Song
College of Optical Science and Engineering
Zhejiang University
Hangzhou, China
zjujintaosong@zju.edu.cn

Shi Zhao
State Key Laboratory for Modern Optical Instrumentation, Center for Optical and Electromagnetic Research, International Research Center for Advanced Photonics, College of Optical Science and Engineering
Zhejiang University
Hangzhou, China
zhaoshi@zju.edu.cn

Wenlei Li
State Key Laboratory for Modern Optical Instrumentation, Center for Optical and Electromagnetic Research, International Research Center for Advanced Photonics, College of Optical Science and Engineering
Zhejiang University
Hangzhou, China
liwenlei@zju.edu.cn

Yaocheng Shi
State Key Laboratory for Modern Optical Instrumentation, Center for Optical and Electromagnetic Research, International Research Center for Advanced Photonics, College of Optical Science and Engineering
Zhejiang University
Hangzhou, China
yaocheng@zju.edu.cn

***Abstract*—We propose a waveguide grating antenna fabricated on the LNOI platform. The side-wall emission can be significantly depressed by building periodical subwavelength structures, leading to large aperture size and an ultrasmall divergence angle of 0.0062°.**

Keywords—optical antenna, Lithium niobate, waveguide grating, integrated photonics

I. Introduction

As the requirement for on-chip beam steering schemes increases, optical phased array (OPA) has drawn significant attention, for its low cost, compactness, high speed, and reliability [1]. Therefore, it has various applications, like light detection and ranging, long-distance imaging, and free-space data communication [2, 3]. OPA enables directional emission by launching phase-controlled beams from nanophotonic antenna arrays. Meanwhile, the divergence angle is an important evaluation indicator of the OPA system. Thus, in recent years, various antenna solutions for narrowing divergence angles have been proposed. However, there are only a few methods considering reducing the side-wall emission loss of the antenna to increase the aperture size of antennas, leading to ultrasmall divergence angles [4, 5]. Furthermore, the diffraction angle can be steered by adjusting the working wavelength commonly. But the diffraction intensity of the antenna is sensitive to the wavelength, so there will be deviations in the transmission power and far-field divergence during the beam steering process, making the scanning operation unstable.

Most of the reported OPA systems are based on the silicon-on-insulator (SOI) platform [6-8]. It actually has some disadvantages, such as the slow speed of phase control by applying thermo-optic phase shifters. Therefore, the development of Lithium Niobate (LN) material offers a novel way to realize OPA systems. It is a rarely high-performance optical material combining advantageous properties of integrated photonics. The large electro-optic coefficients can control the change of refractive index, which has led to the realization of high-speed electro-optic modulators [9]. Besides, broad transparency in the electromagnetic spectrum ranging from 0.35 to 5.0μm effectively reduces absorption loss. Furthermore, its long-term stability, large scale, and low cost make it commercially available. Due to its rich optical properties, lithium niobate-on-insulator (LNOI) has strong competitiveness in integrated optics. Only a few OPA fabricated on LNOI platforms have been proposed [10-12], most of which focus more on enlarging the field of view and pay less attention to reducing the divergence angle by designing antennas.

In this work, we propose a narrow beam antenna utilizing subwavelength structure based on LNOI waveguides. The subwavelength structures are formed by shallow etched periodical nano-grooves on the side walls of LNOI waveguides. It can significantly depress the losses, leading to a large aperture size together with an ultrasmall divergence angle. Also, the interference effect caused by the structure leads to a flattening of the dispersion curve of the diffracted intensity. In addition, two new degrees of freedom are introduced into diffraction engineering, providing a way for the optimization of antennas on the LNOI platform.

II. Design and Principle

Fig. 1(a) and 1(b) show the principle of the proposed waveguide grating antenna on the LNOI platform, which is a LN waveguide with periodic nano-groove on the side-wall. The device is designed based on the LNOI platform with a LN core layer ($n_o = 2.21, n_e = 2.14, h_{LiNbO3} = 600\ nm, \theta = 70°$), and the buffer layer and cladding layer are chosen to be SiO_2 and PMMA respectively ($n_{SiO2} = 1.45, h_{SiO2} = 2\mu m, n_{PMMA} = 1.49, h_{PMMA} = 2\mu m$). In this paper, only the transverse-electric (TE) polarization is considered. As shown in Fig. 1(c), the fundamental TE mode (TE_0) propagates along the LN waveguide (towards the y-axis), and it can be coupled into radiation modes (E_{Top}, E_{Bottom}, $E_{R(+)}$, $E_{L(+)}$) by the nano grooves. It should also be noted that the grating also excites the scattering modes ($E_{R(-)}$, $E_{L(-)}$) in the LN core region. Therefore, by building the shallow etched structure, the effect between $E_{R(\pm)}$ and $E_{L(\pm)}$ is introduced, leading to significant depression of the side-wall emission.

The work is supported by the National Natural Science Foundation of China (62135011; 62105286); "Pioneer" and "Leading Goose" R&D Program of Zhejiang (2022C01103), the Fundamental Research Funds for the Central Universities.

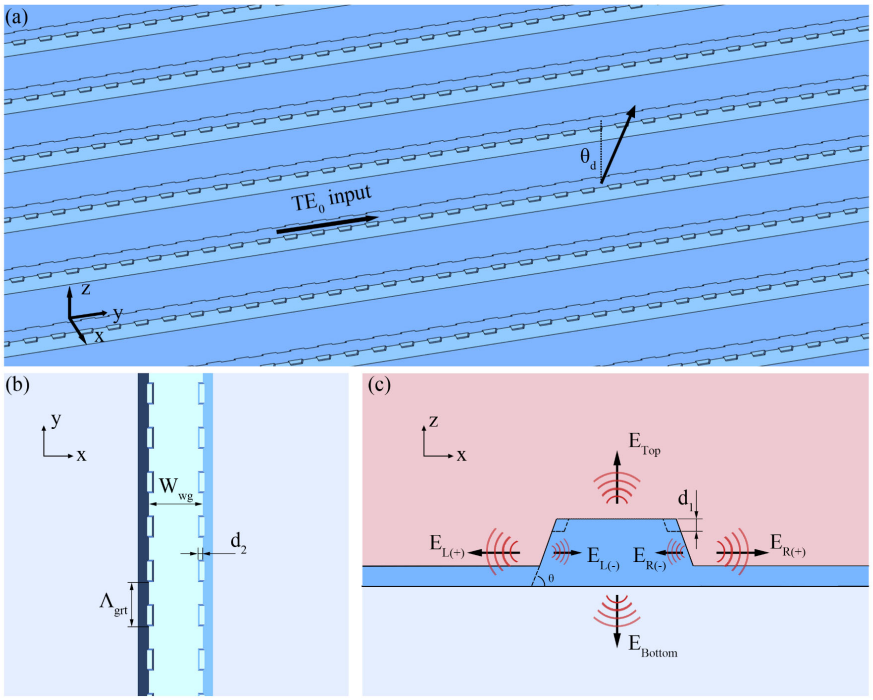

Fig. 1. Schematic and structure diagram of the proposed LN waveguide grating antenna
(a) 3D view of the LN grating antenna. (b) Enlarged top view of $LiNbO_3$ grating antenna with some key parameters labeled. (c) The working principle of the $LiNbO_3$ grating antenna with two key parameters labeled. The fundamental TE mode (TE_0) propagates along the LN waveguide (towards y-axis), and it can be coupled into the radiation mode $(E_{Top}, E_{Bottom}, E_{R(+)}, E_{L(+)})$ by nanogrooves. It should also be noted that, the grating also excites the scattering modes $(E_{R(-)}, E_{L(-)})$ in the LN core region. Therefore, by building the shallow etching structure, the effect between $E_{R(\pm)}$ and $E_{L(\pm)}$ is introduced, leading to significant depression of side-wall emission.

The diffraction formula of the traditional grating antenna [13] is introduced as follows:

$$\kappa = \frac{\Delta n_{eff}}{n_{eff}\Lambda_{grt}} \tag{1}$$

where κ is the coupling coefficient, Δn_{eff} is the effective refractive index difference between the high and the low index sections produced by the grating structure, n_{eff} is the effective refractive index of the grating antenna, Λ_{grt} is the length of the grating period.

However, this formula will no longer apply and will require some modification due to the introduction of d_2, which instigates the bound state in the continuum (BIC) effect as in [14]. And the presence of d_1 results in a shift in the critical waveguide width this effect requires. Thus, the correction can be expressed more intuitively, that is, two new degrees of freedom will be introduced into the diffraction formula, which will provide more optimization methods of diffraction engineering.

And the diffraction angle θ_d of the antenna can be determined as follows:

$$sin\theta_d = n_{eff} - \frac{\lambda_0}{\Lambda_{grt}} \tag{2}$$

where λ_0 is the working wavelength. Then Λ_{grt} is chosen to be $900\,nm$, leading to $\theta_d \approx 15°$ with $1.55\mu m$ as working wavelength.

Also, to verify the effect, the diffraction strength α is defined as:

$$\alpha = \frac{-10\log_{10}(1-S)}{l_{grt}} \tag{3}$$

where S is the radiation power and l_{grt} is the propagation length.

III. Fabrication and Characterzition

We then fabricated LN waveguide grating antennas of different lengths, and measured the diffraction intensity accordingly. To evaluate α, a series of antennas with different propagation length (from 0.4 to 2 mm) and waveguide width (from 660 to 820 nm) were fabricated, as shown in Fig. 2(a). Waveguides without the shallow etching are also fabricated on the same platform for reference. Fig. 2(b) shows the excess losses (EL) for the fabricated antennas with varied propagation length and $W_{wg} = 740nm$ at the $1.55\,\mu m$ wavelength. The excess loss can be determined as follows:

$$EL = -10\log_{10}\left(\frac{T_{WGA}}{T_{wg}}\right) \tag{4}$$

where T_{WGA} is the transmittance of LN waveguide grating antennas, and T_{wg} is the transmittance of the waveguides without shallow etching. We characterized the diffraction intensity as $\alpha \approx 1.77 \times 10^{-3}\ dB/\mu m$ by linearly fitting the experimentally measured excess losses. Fig. 2 (c) shows the experimentally measured α with different W_{wg}. Inevitably, when the width of waveguide approximate 730nm, the measured α achieves a minimum, which agrees well with the simulation results.

To further estimate the proposed LN waveguide grating antenna, we also calculate the divergence angle $\delta\theta_{3dB}$, by predicting the far-field intensities of various different l_{grt}

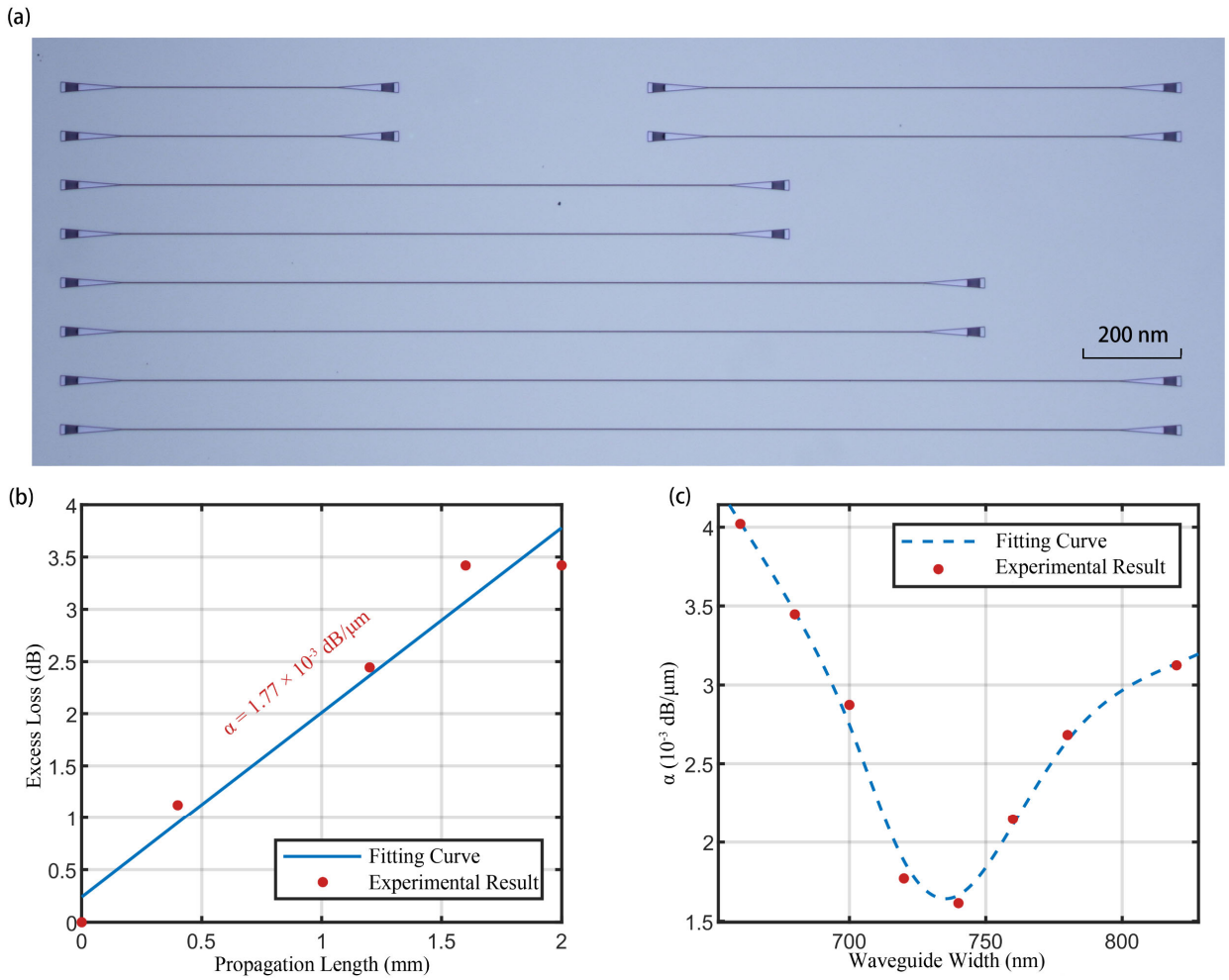

Fig. 2. The fabricated LN waveguide grating antennas and measurement results
(a) Optical microscopy image of fabricated LN waveguide grating antennas and waveguides without shallow etching, with different l_{grt} (from 0.4 to 2 mm) and W_{wg} (from 660 to 820 nm) (b) The excess losses (EL) for fabricated antennas with varied l_{grt} and W_{wg}=720 nm at the 1.55 μm wavelength. The blue line indicates the linear fit. The measured diffraction intensity is $\alpha \approx 1.77 \times 10^{-3}\ dB/\mu m$. (c) The experimentally measured α with different W_{wg}. We found that when the waveguide width is 730 nm, the measured α achieves a minimum.

according to the measured α, as shown in Fig. 3. The calculation detail of the prediction can be found in [15]. For our LN waveguide grating antenna with $W_{wg} = 740\ nm$, the divergence angle decreases with the propagating length varying from 0.5 to 12.5 mm. When the propagating length is taken near the theoretical maximum value, that is, $l_{grt} = 12.5\ mm$, the divergence angle can reach an ultrasmall value of 0.0062°.

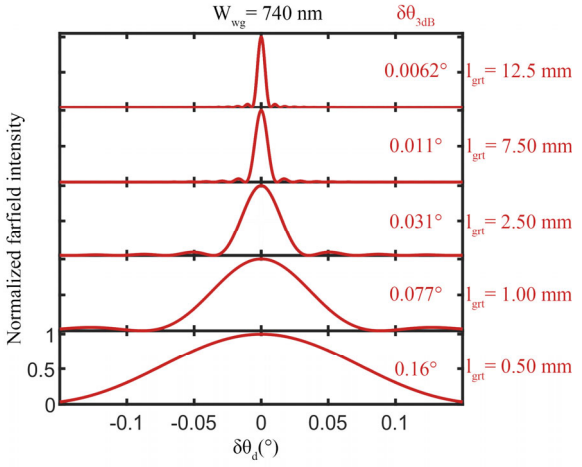

Fig. 3. Predicted far-field intensities for proposed LN waveguide grating antenna with $W_{wg} = 740\ nm\ and$ 1.55μm wavelength. When the propagating length are taken near the theoretical maximum value, that is, $l_{grt} = 12.5\ mm$, the divergence angle can reach an ultrasmall value of 0.0062°.

IV. Conclusion

In conclusion, we have proposed and demonstrated a waveguide grating antenna on the LNOI platform, with an extreme large aperture size of 1.25cm and a ultrasmall divergence angle of 0.0062°. The diffraction strength depresses using the intra waveguide interference. The shallow etched structure can significantly inhibit the launch loss on the side, leading to very weak diffraction strength. Also, two degrees of freedom are introduced into the conventional diffraction formula, offering a novel way for high-performance integrated optical antennas. Moreover, the diffraction strength dispersion can be flattened for waveguide grating antenna at critical waveguide width, which can greatly improve the stability of the OPA system.

References

[1] C.-P. Hsu, B. Li, B. Solano-Rivas, A. R. Gohil, P. H. Chan, A. D. Moore, and V. Donzella, "A review and perspective on optical phased

array for automotive LiDAR," IEEE Journal of Selected Topics in Quantum Electronics, vol. 27, no. 1, pp. 1-16, 2020.

[2] C. V. Poulton, M. J. Byrd, P. Russo, E. Timurdogan, M. Khandaker, D. Vermeulen, and M. R. Watts, "Long-range LiDAR and free-space data communication with high-performance optical phased arrays," IEEE Journal of Selected Topics in Quantum Electronics, vol. 25, no. 5, pp. 1-8, 2019.

[3] H.-W. Rhee, J.-B. You, H. Yoon, K. Han, M. Kim, B. G. Lee, S.-C. Kim, and H.-H. Park, "32 Gbps Data Transmission With 2D Beam-Steering Using a Silicon Optical Phased Array," IEEE Photonics Technology Letters, vol. 32, no. 13, pp. 803-806, 2020.

[4] H. Xu and Y. Shi, "Diffraction engineering for silicon waveguide grating antenna by harnessing bound state in the continuum," Nanophotonics, vol. 9, no. 6, pp. 1439-1446, 2020.

[5] J. Chen, J. Wang, J. Li, Y. Yao, Y. Sun, J. Tian, Y. Zou, X. Zhao, and X. Xu, "Subwavelength structure enabled ultra-long waveguide grating antenna," Optics Express, vol. 29, no. 10, pp. 15133-15144, 2021.

[6] J. Sun, E. Timurdogan, A. Yaacobi, E. S. Hosseini, and M. R. Watts, "Large-scale nanophotonic phased array," Nature, vol. 493, no. 7431, pp. 195-199, 2013.

[7] K. Van Acoleyen, H. Rogier, and R. Baets, "Two-dimensional optical phased array antenna on silicon-on-insulator," Optics express, vol. 18, no. 13, pp. 13655-13660, 2010.

[8] S. Chung, H. Abediasl, and H. Hashemi, "15.4 A 1024-element scalable optical phased array in 0.18 μm SOI CMOS," in 2017 IEEE International Solid-State Circuits Conference (ISSCC). IEEE, 2017, pp. 262-263.

[9] J. Cai, C. Guo, C. Lu, A. P. T. Lau, P. Chen, and L. Liu, "Design optimization of silicon and lithium niobate hybrid integrated traveling-wave Mach-Zehnder modulator," IEEE Photonics Journal, vol. 13, no. 4, pp. 1-6, 2021.

[10] S. Tan, J. Liu, Y. Liu, H. Li, Q. Lu, and W. Guo, "Two-dimensional beam steering based on LNOI optical phased array," in CLEO: Science and Innovations. Optica Publishing Group, 2020, pp. SM2M-1.

[11] Z. Wang, J. Ji, X. Ye, Y. Chen, X. Li, W. Song, B. Fang, J. Chen, S. Zhu, and T. Li, "On-chip integration of metasurface-doublet for optical phased array with enhanced beam steering," Nanophotonics, 2023.

[12] Z. Wang, W. Song, Y. Chen, B. Fang, J. Ji, H. Xin, S. Zhu, and T. Li, "Metasurface empowered lithium niobate optical phased array with an enlarged field of view," Photon. Res., vol. 10, no. 11, pp. B23-B29, 2022.

[13] K. Shang, C. Qin, Y. Zhang, G. Liu, X. Xiao, S. Feng, and S. Yoo, "Uniform emission, constant wavevector silicon grating surface emitter for beam steering with ultra-sharp instantaneous field-of-view," Optics Express, vol. 25, no. 17, pp. 19655-19661, 2017.

[14] C.-L. Zou, J.-M. Cui, F.-W. Sun, X. Xiong, X.-B. Zou, Z.-F. Han, and G.-C. Guo, “Guiding light through optical bound states in the continuum for ultrahigh-Q microresonators,” Laser & Photonics Reviews, vol. 9, no. 1, pp. 114–119, 2015.

[15] W. Xie, J. Huang, T. Komljenovic, L. Coldren, and J. Bowers, "Diffraction limited centimeter scale radiator: metasurface grating antenna for phased array LiDAR," arXiv preprint arXiv:1810.00109, 2018.